Statistical Characterization of GLONASS Broadcast Ephemeris Errors

Liang Heng, Grace Xingxin Gao, Todd Walter, and Per Enge,
Stanford University

BIOGRAPHY

Liang Heng is a Ph.D. candidate under the guidance of Professor Per Enge in the Department of Electrical Engineering at Stanford University. He received his B.S. and M.S. degrees in electrical engineering from Tsinghua University, Beijing, China. His current research interests include GNSS integrity and modernization.

Grace Xingxin Gao, Ph.D., is a research associate in the GPS lab of Stanford University. She received the B.S. degree in mechanical engineering and the M.S. degree in electrical engineering, both at Tsinghua University, Beijing, China. She obtained the Ph.D. degree in electrical engineering at Stanford University. Her current research interests include GNSS signal and code structures, GNSS receiver architectures, and interference mitigation. She has received the Institute of Navigation (ION) Early Achievement Award.

Todd Walter, Ph.D., is a senior research engineer in the Department of Aeronautics and Astronautics at Stanford University. He received his Ph.D. from Stanford and is currently working on the Wide Area Augmentation System (WAAS), defining future architectures to provide aircraft guidance, and working with the FAA and GPS Wing on assuring integrity on GPS III. Key early contributions include prototype development proving the feasibility of WAAS, significant contribution to WAAS MOPS, and design of ionospheric algorithms for WAAS. He is a fellow of the Institute of Navigation.

Per Enge, Ph.D., is a Professor of Aeronautics and Astronautics at Stanford University, where he is the Kleiner-Perkins, Mayfield, Sequoia Capital Professor in the School of Engineering. He directs the GPS Research Laboratory, which develops satellite navigation systems based on the Global Positioning System (GPS). He has been involved in the development of WAAS and LAAS for the FAA. Per has received the Kepler, Thurlow and Burka Awards from the ION for his work. He is also a Fellow of the ION and the Institute of Electrical and Electronics Engineers (IEEE). He received his PhD from the University of Illinois in 1983.

ABSTRACT

For critical navigation applications such as aircraft approach and landing, there is a general desire to use multi-constellation global navigation satellite systems (GNSS) to enhance availability and reliability. The Russian Global Navigation Satellite System (GLONASS) is so far the only other constellation nearly as developed as the Global Positioning System (GPS). A thorough characterization of GLONASS signal-in-space errors is beneficial to not only the GLONASS users but also the development of next-generation multi-constellation GNSS integrity monitoring systems such as advanced receiver autonomous integrity monitoring.

In this paper, we characterize the nominal GLONASS ephemeris errors (without counting in clock errors) based on the data in the past three years. The ephemeris errors are computed by comparing broadcast ephemerides with precise ones, both of which were obtained from International GNSS Service. The formula for GLONASS global-average rms user range error (URE) has been derived. Anomalous satellite behaviors and bad receiver data are excluded by an outlier filter. Ephemeris errors are characterized with respect to long-term stationarity, resultant user range errors (UREs), mean, spatial correlation, and distribution. The results show that GLONASS broadcast ephemerides have achieved stable sub-meter orbital accuracy, and the traditional assumption of spatial-independent zero-mean Gaussian distribution is not generally valid for ephemeris errors.

INTRODUCTION

The Russian Global Navigation Satellite System (GLONASS) is so far the only fully developed global navigation satellite system (GNSS) other than the United States' Global Positioning System (GPS). At the time of writing, 23 GLONASS satellites are operational [1] and capable of global continuous navigation [2]. A combination of GPS

and GLONASS can enhance availability and reliability with better satellite geometries and more redundant observation data, especially for high latitude users [3, 4] and the use of receiver autonomous integrity monitoring (RAIM) [5, 6].

Both GLONASS and GPS employ the concept of trilateration, in which the measured distance from a user receiver to at least four satellites in view as well as the positions and clocks of these satellites are the prerequisites for the user receiver to fix its exact position [7]. For most users, real-time satellite positions and clocks are derived from ephemeris parameters and clock correction terms in broadcast navigation messages, which are generated by the control segment (CS) on the basis of a prediction model and the measurements at several monitor stations [2, 8]. The differences between the broadcast ephemerides/clocks and the truth account for signal-in-space (SIS) errors, which directly affect the positioning accuracy and integrity. Knowledge about SIS errors is important not only for assessing the system performance but also for developing the next generation multi-constellation GNSS integrity monitoring system.

Usually, SIS performance are evaluated with respect to accuracy and integrity. SIS accuracy is more related to nominal SIS errors, whereas integrity is more related to anomalous SIS errors. For GPS, the nominal SIS errors have been extensively studied in [9–14], and the anomalous SIS errors have been studied in [12, 13, 15–19]. For GLONASS, although there have been some relevant prior work [20–22], a thorough study of nominal and anomalous SIS errors is of great need. This paper focuses on the statistical characterization of nominal GLONASS ephemeris errors (without counting in clock errors), taking the first step to a complete characterization of GLONASS SIS errors.

This paper employs a methodology similar to [14]. Ephemeris errors are computed by comparing the broadcast orbits with the precise ones, and then are characterized with respect to long-term stationarity, resultant user range errors (UREs), mean, spatial correlation, and distribution. For the rest of this paper, we start with a description of the data sources. Then, we elaborate on the methodology. Finally, we present the statistics of the GLONASS ephemeris errors over the past three years.

DATA SOURCES

Broadcast ephemerides

GLONASS broadcast navigation message data are publicly available at International GNSS Service (IGS) [23]. These data are archived in receiver independent exchange (RINEX) n-type format [24], which include the immediate information in the broadcast navigation message such as reference time, clock correction, satellite position, satellite velocity, and lunisolar acceleration [25].

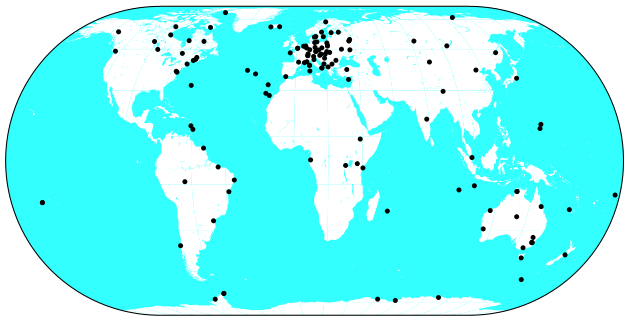

Figure 1. IGS GPS/GLONASS stations as of Jan 30, 2011 (adapted from `http://igscb.jpl.nasa.gov`)

As shown in Figure 1, IGS tracking network comprises more than 100 GPS/GLONASS stations all over the world to ensure seamless, redundant data logging. Since broadcast navigation messages are usually updated every 30 minutes, no single station can collect all navigation messages. For ease of using, an IGS archive site, Crustal Dynamics Data Information System (CDDIS), routinely generates daily global combined broadcast navigation message data files `brdc`*`ddd`*`0.yyg` (or `igex`*`ddd`*`0.yyg` before December 2004) [26]. Unfortunately, these files sometimes contain errors. For example, the reference time t_b in GLONASS broadcast ephemerides is always an integer multiple of 15 minutes [25], but we observe the following lines in `brdc0020.09g`:

```
 4 09  1  2  0 15  0.0 0.119622796774E-03...
 4 09  1  2  0 15  1.0 0.119622796774E-03...
```

The first line indicates an ephemeris with t_b = 2009-01-02 00:15:00, whereas the second line indicates an ephemeris with the same parameters as the first one but an invalid t_b = 2009-01-02 00:15:01.

A simple solution to this specific problem is to remove the ephemerides without valid t_b. Besides, there may be other kinds of errors caused by ground receiver or data archive process, and a data cleansing algorithm similar to the one proposed in [18, 19] is able to correct these errors. Nevertheless, in this paper we skip this step because we focus on nominal meter-level ephemeris errors, and the data errors usually result in ephemeris errors of several kilometers or more, which can be easily excluded by the outlier filter described in the next section.

Precise ephemerides

In addition to broadcast navigation message data, IGS provides GLONASS precise ephemerides since at least 1999. Derived from the post-process of observation data, precise

ephemerides have an accuracy of 5 centimeters [27] and hence are regarded as ground truth in this paper. To compare the broadcast ephemerides with the precise ones, we need to pay attention to the following issues.

First, precise ephemerides are available at 15-minute intervals synchronized to GPS time, whereas the reference time of broadcast ephemerides is synchronized to GLONASS time. Regardless of the fixed three-hour difference between GLONASS time and Coordinated Universal Time (UTC) [25], the difference between GPS time and GLONASS time includes the leap seconds (between UTC and GPS) and a sub-second bias τ_{GPS} [25]. In this paper, only the leap seconds are taken into account because τ_{GPS} is usually less than one microsecond and the resulting ephemeris error is less than 4 millimeters.

The second issue is that broadcast ephemerides are based on the "Earth Parameters 1990" (PZ-90) coordinate datum, which was not fully consistent with the International Terrestrial Reference Frame (ITRF) used by precise ephemerides [28]. Since September 2007, an improved datum PZ-90.02 has been implemented and the users are recommended to use zero transformation parameters [29]. Therefore, a reference system transformation is not considered necessary in this paper.

The third issue is that the IGS precise ephemerides are based on the measurement of satellite center of mass (CoM). Since the broadcast ephemerides are based on antenna phase center (APC), the CoM data must be converted into APC before being used. In this paper, the antenna corrections provided by IGS [30,31] are used to convert the CoM precise ephemerides into APC.

Last but not least, IGS does not provide GLONASS precise clock data [27]. Therefore, this paper considers only the SIS errors due to broadcast ephemeris errors with an assumption of zero clock errors.

METHODOLOGY

Figure 2 shows the framework of the whole process. According to the discussion on the data sources in the previous section, we firstly remove the invalid items in the broadcast ephemerides and then propagate them at 15-minute intervals synchronized to the precise ephemerides. The precise ephemerides are converted from CoM to APC, and the difference between the propagated broadcast ephemerides and the precise ephemerides in APC are the raw ephemeris errors in the Earth-Centered, Earth-Fixed (ECEF) coordinate. Next, the ephemeris errors in space vehicle coordinate as well as the SIS URE are computed, followed by outlier filtering and robust statistics. The algorithms used in each step will be explained in detail in the following subsections.

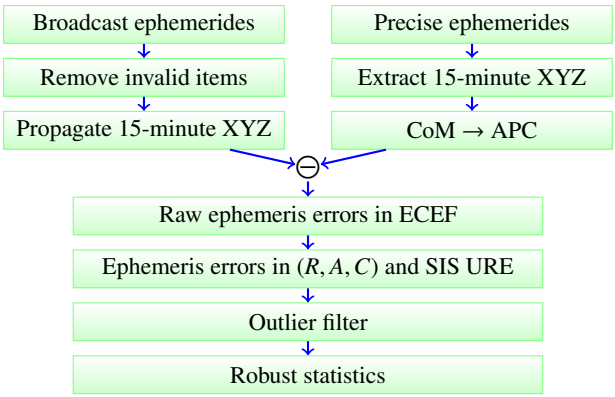

Figure 2. Framework of the whole process

Broadcast ephemeris propagation

While GPS and Galileo broadcast Keplerian ephemeris parameters, GLONASS broadcasts relatively raw Cartesian ephemeris parameters which consists of the instantaneous satellite position, satellite velocity, and lunisolar acceleration in ECEF at a reference time t_b. In this paper, we use the force model recommended by GLONASS ICD[1] to propagate the satellite position at time t, $|t - t_b| \leq 15$ minutes:

$$\ddot{x} = \eta_1 x + \eta_2(1 - \eta_3)x + \omega^2 x + 2\omega\dot{y} + \ddot{x}_{LS}, \quad (1)$$

$$\ddot{y} = \eta_1 y + \eta_2(1 - \eta_3)y + \omega^2 y - 2\omega\dot{x} + \ddot{y}_{LS}, \quad (2)$$

$$\ddot{z} = \eta_1 z + \eta_2(3 - \eta_3)z + \ddot{z}_{LS}. \quad (3)$$

In the above equations, $\eta_1 = -GM/r^3$ accounts for the gravity; $\eta_2 = -1.5J_2GMa_e^2/r^5$ and $\eta_3 = 5z^2/r^2$ account for the perturbation due to Earth oblateness; ω is the Earth rotation rate; $\ddot{x}_{LS}$, $\ddot{y}_{LS}$, and $\ddot{z}_{LS}$ are the lunisolar acceleration given by the broadcast ephemeris. A more thorough discussion of these equations can be found in [25, 32].

Following the recommendation in [25,33], we use the fourth-order Runge-Kutta method with 50-second step to propagate broadcast ephemerides at the 15-minute intervals that coincide with the precise ones. The resulting numerical integration errors are expected to be less than 1 millimeter at $t_b \pm 20$ minutes [33].

SIS error metrics

The broadcast and precise ephemerides mentioned above are in ECEF coordinate, so are the ephemeris errors. Greater insight can be provided if the ephemeris errors are represented in the reference frame with respect to the space vehicle: R—radial, A—alongtrack, and C—crosstrack. Besides, we use T to denote the broadcast clock error.

For an arbitrary set of values for (R, A, C, T), GLONASS

[1]The equations given by [25] have a few typos. Equations (1)–(3) are adapted from [32].

receivers at different locations on the Earth may experience different UREs. Appendix shows that the global-average rms URE is given by

$$\text{rms URE} = \sqrt{(0.98R - T)^2 + (A^2 + C^2)/45}. \quad (4)$$

Due to the lack of precise clock data, in this paper we consider the orbit-error-only global-average rms URE

$$\text{rms URE}_\text{O} = \sqrt{(0.98R)^2 + (A^2 + C^2)/45}. \quad (5)$$

Outlier filter

As mentioned in the previous section, broadcast ephemeris data may contain errors caused in data logging. In addition, the broadcast and the precise ephemerides have some build-in features to indicate "unhealthy" or "something happened". Therefore, the following outlier filters are used in this paper:

- Broadcast ephemerides: check health bits;
- Precise ephemerides: check event flags;
- Check if global-average rms URE_O greater than 50 meters.

Because the RINEX format for GLONASS navigation messages does not include an important parameter, user range accuracy, we have to choose a fixed threshold: 50 meters. One reason for this threshold is from our observation that during the past three years apparent anomalies generally caused URE_O greater than 50 meters. Moreover, the average URE_O is usually around 1 meter, and a 50-meter threshold is conservative enough to avoid excluding nominal ephemeris errors.

Robust statistics

Since ephemeris errors do not necessarily have a normal distribution, the traditional statistics such as mean, standard deviation, and correlation coefficient may be affected by some extreme samples. To cope with this problem, we use trimmed mean (also referred to as truncated mean) to measure the central tendency. A trimmed mean function $\text{mean}_\alpha(\cdot)$ is the mean after discarding the samples at the $50\alpha\%$ high end and $50\alpha\%$ low end. Analogously, a trimmed standard deviation function is defined as

$$\text{std}_\alpha(X) = \sqrt{\text{mean}_\alpha((X - \text{mean}_\alpha(X))^2)}. \quad (6)$$

In fact, a trimmed mean is a compromise between a mean and a median, and a trimmed standard deviation a compromise between a standard deviation and a median absolute deviation. In this paper, we use a small value $\alpha = 0.05$, i.e., use 95% of the data, to make the trimmed mean close to the mean and the trimmed standard deviation close to the standard deviation.

As for the measure of statistical independence, we employ Spearman's rank correlation coefficient as a robust estimator. The details about this method can be found in some statistics textbooks such as [34].

Normality metric

Ephemeris errors are usually described or overbounded by a normal distribution. Hence, it is important to know how close the real errors are to normally distributed. Popular statistical hypothesis tests of normality, such as Jarque-Bera test, Shapiro-Wilk test, and Lilliefors test [35], usually reject the null hypothesis that the ephemeris errors comes from a distribution in the normal family. Even worse, common software implementations of these tests can seldom return a meaningful p-value [36] to tell how far ephemeris error samples are from normally distributed. Therefore, we use kurtosis to quantify normality. Kurtosis (or excess kurtosis) is defined as

$$\gamma(X) = \frac{\mathbb{E}(X - \mathbb{E}X)^4}{\left(\mathbb{E}(X - \mathbb{E}X)^2\right)^2} - 3. \quad (7)$$

A normal distribution has kurtosis $\gamma = 0$; a sub Gaussian distribution with light tails usually has kurtosis $\gamma < 0$; a super Gaussian distribution with heavy tails usually has kurtosis $\gamma > 0$.

Since kurtosis involves 4th-order statistics, it relies on extreme values but is vulnerable to statistical outliers. The "trimmed" method, discarding a certain percent of extreme samples, works well for the mean and the standard deviation but introduces a significant bias for kurtosis. Alternatively, we compute kurtosis after discarding the samples with the absolute value greater than 6 times interquartile range. For a normal distribution, 6 times interquartile range is approximately equal to 8-sigma, equivalent to 1.2×10^{-15} tail probability. Because the sample size is less than 10^5 for each satellite, this tail probability ensures that only statistical outliers are discarded. This feature is important to a correct kurtosis estimation.

STATISTICAL CHARACTERIZATION

Long-term stationarity

Before calculating any statistics, we first verify if the data used in this study are stationary. Figure 3 shows the daily rms R, A, C, and orbit-error-only URE for two GLONASS satellites. The performance of GLONASS-M 721 was stationary during the past three years and a similar performance can be seen for all other GLONASS satellites except GLONASS-M 727, whose ephemeris performance showed an unusual jump in September 2009. For the ease of programming and the sake of a "fair" comparison, the statistics in this paper will be based on the data from 2009-01-01 to 2011-08-27 (969 days). The results of GLONASS-M

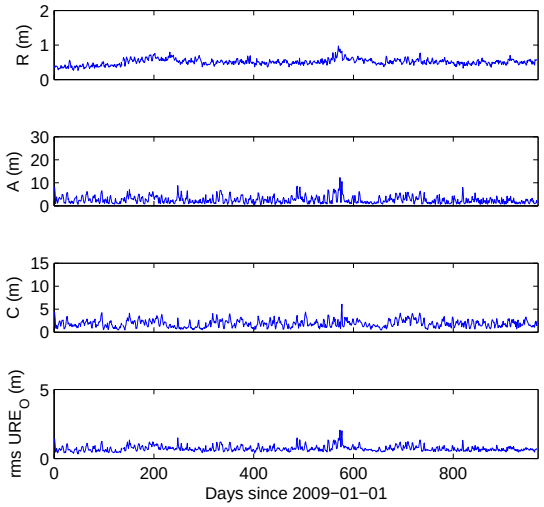

(a) Typical long-term performance: GLONASS-M 721

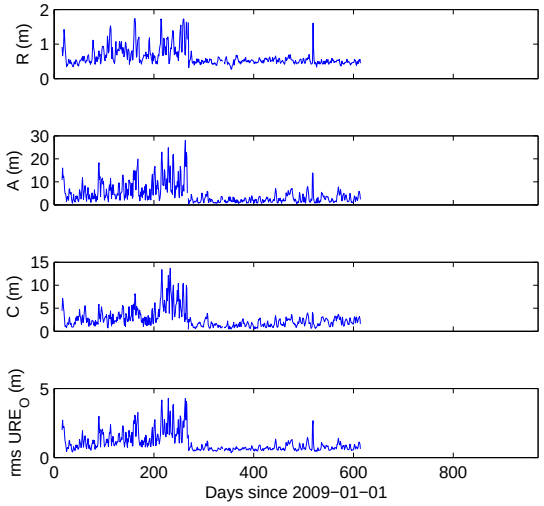

(b) Atypical long-term performance: GLONASS-M 727

Figure 3. Daily rms R, A, C, and orbit-error-only URE

727 are only for reference purpose, not only because of its non-stationary behavior, but also because this satellite has been in maintenance since September 2010.

Global-average rms URE$_O$

Figure 4 compares the orbit-error-only global-average rms URE$_O$ over the past three years. The satellites are arranged chronologically according when they were launched. For example, GLONASS-M 712 launched in December 2004 is the oldest, and GLONASS-M 736–738 launched in September 2010 are the youngest. It should be noted that a few old satellites such as GLONASS-M 713, 718, and 726 were removed from service one or two years ago.

One purpose of Figure 4 is to show that most GLONASS satellites have achieved sub-meter user range accuracy (with assuming zero clock errors), which is comparable to, although not as good as, the orbit-error-only global-average rms URE$_O$ of GPS [14]. Another purpose of this figure is to double check the assumption of stationarity. Clearly, all satellites except GLONASS-M 727 showed a stable rms URE$_O$ performance during the past three years.

Figure 5 compares the orbit-error-only global-average rms URE$_O$ of different propagation distances. As expected, the

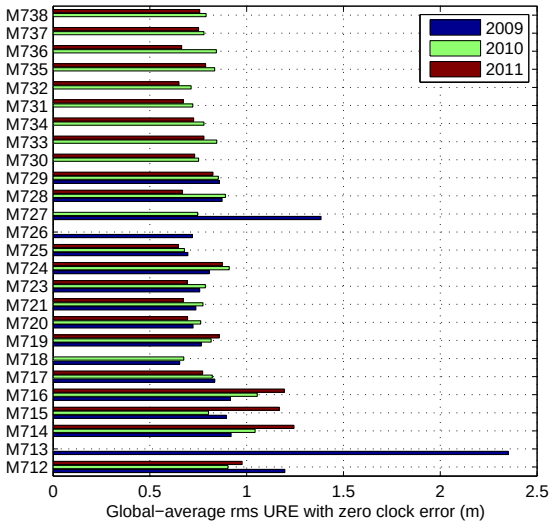

Figure 4. Orbit-error-only global-average rms URE$_O$ in 2009, 2010, and 2011

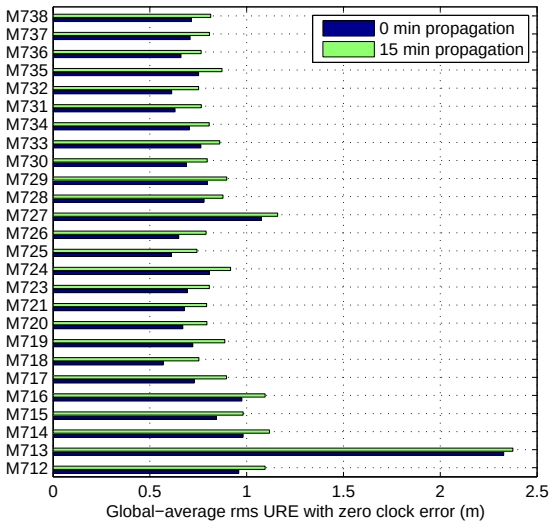

Figure 5. Orbit-error-only global-average rms URE$_O$ for 0- and 15-minute propagation

0-minute propagation (actually 15 seconds due to the leap seconds) exhibits a smaller error. The 15-minute propagation results in on average 0.13-meter degradation. This may be a particular problem with the GLONASS Cartesian ephemeris format and the recommended force model [25]; we haven't observed any similar problem with the GPS Keplerian ephemeris format.

Mean of ephemeris errors

Although ephemeris errors are generally assumed to be zero-mean distributed, the reality may be different. Figure 6 shows the mean of R, A, and C normalized by the standard deviation. In Figure 6, the red dots denote the mean, while the blue lines with a length of twice the standard deviation are centered at the red dots.

Figure 6 indicates that a zero-mean assumption for the crosstrack errors is generally valid. However, the alongtrack errors usually have a negative mean. Even worse, the radial errors of the younger satellites usually have a negative mean and the amplitude of the mean is as large as the standard deviation. We are not sure if this is a problem due to the GLONASS system or the CoM-to-APC correction parameters provided by IGS. Actually, IGS CoM-to-APC correction parameters for GPS have a similar problem [19].

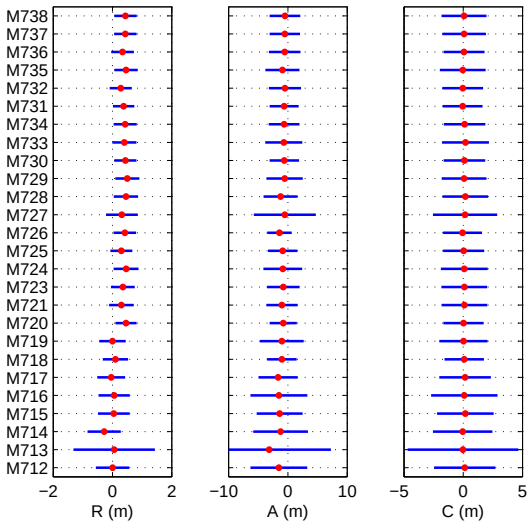

Figure 6. Mean of ephemeris errors with a comparison to standard deviation. The blue line with a length of twice the standard deviation is centered at the mean denoted by the red dot.

Spatial correlation of ephemeris errors

The three components of ephemeris error, R, A, and C, are not necessarily independent from each other. We computed the Spearman's rank correlation coefficients [34] for every pair among R, A, and C. As shown in Figure 7, the correlation $\langle R, A\rangle$ and $\langle A, C\rangle$ are not obvious because most of the satellites have a correlation coefficient with an amplitude less than 0.1. However, a negative correlation between R and A is very common. The correlation $\langle R, A\rangle$ is mainly due to the conservation of angular momentum (in an Earth-centered inertial frame): $\boldsymbol{r} \times \boldsymbol{v}$ = constant, where $\boldsymbol{r}$ is the vector from the earth to a satellite, and $\boldsymbol{v}$ is the velocity of the satellite. Therefore, an overestimate of R results in an underestimate of $|\boldsymbol{v}|$, which usually leads to an underestimate of C. Interestingly, GPS also shows a significant negative correlation between R and A, but the correlation coefficient is around -0.35 [14], roughly as twice large as the correlation coefficient observed in GLONASS.

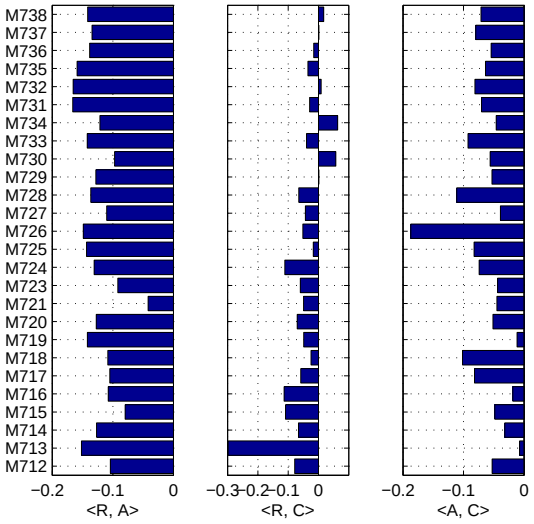

Figure 7. Correlation coefficients among radial errors, alongtrack errors, and crosstrack errors

Distribution of ephemeris errors

Figure 8 shows the kurtosis of radial, alongtrack, and crosstrack ephemeris errors for all GLONASS satellites. It can be seen that super Gaussian distribution is the most common, especially for radial and alongtrack errors. GPS ephemeris errors exhibit similar behavior but not to such an extent [14].

For a more intuitive understanding of the distribution of ephemeris errors, Figure 9 shows the Q-Q plots of GLONASS-M 714 radial errors and GLONASS-M 721 crosstrack errors. The former represents a typical super Gaus-

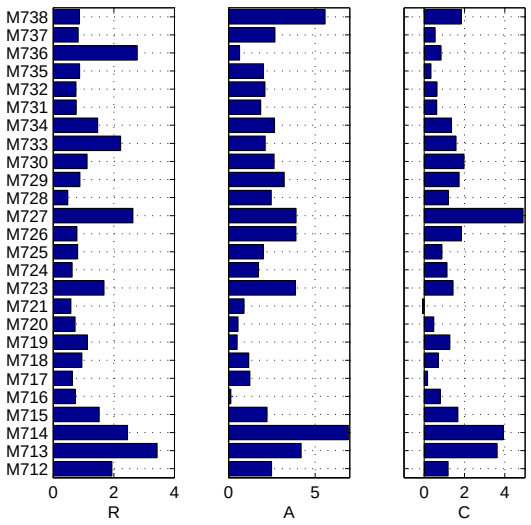

Figure 8. Kurtosis of ephemeris errors. Positive value indicates a super Gaussian distribution with heavy tails.

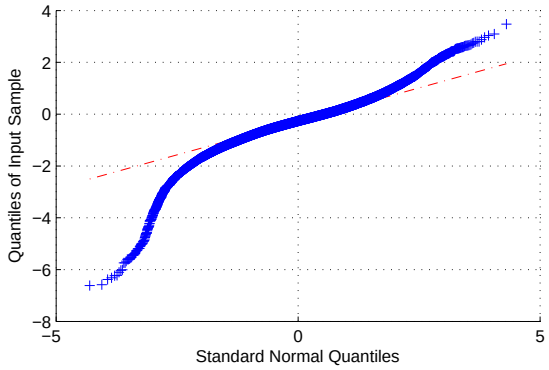

(a) GLONASS-M 714 radial errors
($\gamma = 2.45$, super Gaussian, typical)

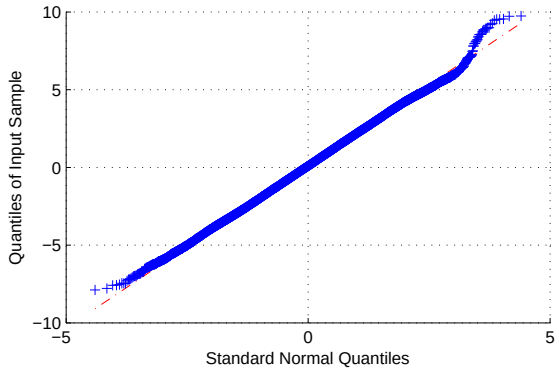

(b) GLONASS-M 721 crosstrack errors
($\gamma = -0.08$, Gaussian, atypical)

Figure 9. Q-Q plots of the ephemeris errors of two satellites

sian distribution, whereas the latter represents an atypical Gaussian distribution. We observed that not only most of ephemeris errors have very heavy tails, but sometimes the distribution of tails are also asymmetric. In practice, a normal distribution with inflated sigma may be used to overbound ephemeris errors, or a more sophisticated distribution [14, 37] should be considered.

SUMMARY

In this paper, we characterized GLONASS broadcast ephemeris errors with respect to long-term stationarity, resultant UREs, mean, spatial correlation, and distribution. The ephemeris errors are computed by comparing broadcast ephemerides with precise ones, both of which are obtained from IGS. The global-average rms URE for GLONASS is derived and computed. The long-term analysis shows that the GLONASS ephemeris performance was stationary over the past 969 days from 2009-01-01 to 2011-08-27. The evaluation of global-average rms URE shows that GLONASS achieved stable sub-meter orbit-error-only user range accuracy over the past three years, and the 15-minute ephemeris propagation leads to 0.13-meter degradation. The mean analysis shows that some satellites have obvious nonzero mean for radial and alongtrack errors. The distribution analysis shows that radial and alongtrack errors usually have a super Gaussian distribution. We hope that the results presented in this paper will help GLONASS users and the development of multi-constellation GNSS integrity monitoring systems.

APPENDIX

The global-average rms URE shown in (4) can be derived as follows. Assume the Earth is a perfect sphere with a normalized radius 1. Without loss of generality, assume the true position of the satellite is $(0, 0, r)$ in ECEF, where r is the normalized distance between the satellite and the center of the Earth. Then, the instantaneous URE of the receiver at latitude θ, longitude ϕ, and height 0 is given by

$$\text{I URE} = (R, A, C) \cdot \mathbf{1}, \tag{8}$$

where $\cdot$ is the vector dot product, R is the radial error, A is the alongtrack error, C is the crosstrack error, and $\mathbf{1}$ is the normalized vector from the receiver to the satellite

$$\mathbf{1} = \frac{(-\cos\theta\cos\phi, -\cos\theta\sin\phi, r - \sin\theta)}{\sqrt{1 + r^2 - 2r\sin\theta}}. \tag{9}$$

Therefore, the global-average rms URE can be calculated by

$$\text{rms URE}^2 = \frac{1}{S}\int_{\vartheta}^{\pi/2}\int_{-\pi}^{\pi}(\text{I URE} - T)^2\cos\theta\,\mathrm{d}\theta\mathrm{d}\phi, \tag{10}$$

where T is the clock error, ϑ is the latitude of the edge of the satellite's coverage footprint, and $S = 2\pi(1 - \sin\vartheta)$ is the area of the coverage footprint.

For GLONASS, we have $r = 3.998$ and $\vartheta = 14.48°$ (assuming zero mask angle), and the corresponding global-average rms URE is given by

$$\begin{aligned} &\text{rms URE}^2_{\text{GLONASS}} \\ &= 0.9555R^2 - 1.955RT + T^2 + 0.02224(A^2 + C^2) \\ &\approx (0.98R - T)^2 + (A^2 + C^2)/45, \end{aligned} \quad (11)$$

which is equivalent to (4).

For verification purpose, let us compute the formula for GPS. Using $r = 4.175$ and $\vartheta = 13.85°$, the corresponding global-average rms URE is given by

$$\begin{aligned} &\text{rms URE}^2_{\text{GPS}} \\ &= 0.9593R^2 - 1.959RT + T^2 + 0.02034(A^2 + C^2) \\ &\approx (0.98R - T)^2 + (A^2 + C^2)/49, \end{aligned} \quad (12)$$

which is the same as [38].

ACKNOWLEDGMENTS

The author gratefully acknowledges the support of the Federal Aviation Administration under Cooperative Agreement 08-G-007. This paper contains the personal comments and beliefs of the author, and does not necessarily represent the opinion of any other person or organization.

REFERENCES

[1] GLONASS status, Accessed January 2011. [Online]. Available: http://www.glonass-ianc.rsa.ru/pls/htmldb/f?p=202:20:3899835789065754::NO:::

[2] S. Revnivykh, "GLONASS status and progress," in *Proceedings of the 23rd International Technical Meeting of The Satellite Division of the Institute of Navigation (ION GNSS 2010)*, Portland, OR, September 2010, pp. 609–633.

[3] S. Dosso, M. Vinnins, G. Lachapelle, G. Heard, and E. Cannon, "High latitude attitude," *GPS World*, October 2003.

[4] G. X. Gao, L. Heng, T. Walter, and P. Enge, "Breaking the ice: Navigating in the arctic," in *Proceedings of the 24th International Technical Meeting of The Satellite Division of the Institute of Navigation (ION GNSS 2011)*, Portland, OR, September 2011.

[5] S. Hewitson and J. Wang, "GNSS receiver autonomous integrity monitoring (RAIM) performance analysis," *GPS Solutions*, vol. 10, pp. 155–170, 2006.

[6] M. Choi, J. Blanch, D. Akos, L. Heng, G. Gao, T. Walter, and P. Enge, "Demonstrations of multi-constellation advanced raim for vertical guidance using gps and glonass signals," in *Proceedings of the 24th International Technical Meeting of The Satellite Division of the Institute of Navigation (ION GNSS 2011)*, Portland, OR, September 2011.

[7] P. Misra and P. Enge, *Global Positioning System: Signals, Measurements, and Performance*, 2nd ed. Lincoln, MA: Ganga-Jamuna Press, 2006.

[8] T. Creel, A. J. Dorsey, P. J. Mendicki, J. Little, R. G. Mach, and B. A. Renfro, "Summary of accuracy improvements from the GPS legacy accuracy improvement initiative (L-AII)," in *Proceedings of the 20th International Technical Meeting of the Satellite Division of The Institute of Navigation (ION GNSS 2007)*, Fort Worth, TX, September 2007, pp. 2481–2498.

[9] J. Zumberge and W. Bertiger, "Ephemeris and clock navigation message accuracy," in *Global Positioning System: Theory and Applications*, B. Parkinson, J. Spilker, P. Axelrad, and P. Enge, Eds. Washington, DC: American Institute of Aeronautics and Astronautics, 1996, vol. I, pp. 585–699.

[10] R. B. Langley, H. Jannasch, B. Peeters, and S. Bisnath, "The GPS broadcast orbits: an accuracy analysis," in *33rd COSPAR Scientific Assembly*, Warsaw, Poland, July 2000.

[11] D. M. Warren and J. F. Raquet, "Broadcast vs. precise GPS ephemerides: a historical perspective," *GPS Solutions*, vol. 7, pp. 151–156, 2003.

[12] T. Walter, J. Blanch, and P. Enge, "Evaluation of signal in space error bounds to support aviation integrity," in *Proceedings of the 22nd International Technical Meeting of The Satellite Division of the Institute of Navigation (ION GNSS 2009)*, Savannah, GA, September 2009, pp. 1317–1329.

[13] J. C. Cohenour and F. van Graas, "GPS orbit and clock error distributions," *NAVIGATION, Journal of the Institute of Navigation*, acceptted April 2009.

[14] L. Heng, G. X. Gao, T. Walter, and P. Enge, "Statistical characterization of GPS signal-in-space errors," in *Proceedings of the 2011 International Technical Meeting of the Institute of Navigation (ION ITM 2011)*, San Diego, CA, January 2011.

[15] K. Kovach, J. Berg, and V. Lin, "Investigation of upload anomalies affecting IIR satellites in October 2007," in *Proceedings of the 21st International Technical Meeting of the Satellite Division of The Institute of Navigation (ION GNSS 2008)*, Savannah, GA, September 2008, pp. 1679–1687.

[16] J. Lee, "Results on test of URA validation protocol using NGA data," in *GEAS Working Group*, May 2009.

[17] G. X. Gao, H. Tang, J. Blanch, J. Lee, T. Walter, and P. Enge, "Methodology and case studies of signal-in-space error calculation top-down meets bottom-up," in *Proceedings of the 22nd International Technical Meeting of The Satellite Division of the Institute of Navigation (ION GNSS 2009)*, Savannah, GA, September 2009, pp. 2824–2831.

[18] L. Heng, G. X. Gao, T. Walter, and P. Enge, "GPS ephemeris error screening and results for 2006–2009," in *Proceedings of the 2010 International Technical Meeting of the Institute of Navigation (ION ITM 2010)*, San Diego, CA, January 2010, pp. 1014–1022.

[19] ——, "GPS signal-in-space anomalies in the last decade: Data mining of 400,000,000 GPS navigation messages," in *Proceedings of the 23rd International Technical Meeting of The Satellite Division of the Institute of Navigation (ION GNSS 2010)*, Portland, OR, September 2010, pp. 3115–3122.

[20] E. G. Oleynik, V. V. Mitrikas, S. G. Revnivykh, A. I. Serdukov, E. N. Dutov, and V. F. Shiriaev, "High-accurate GLONASS orbit and clock determination for the assessment of system performance," in *Proceedings of the 19rd International Technical Meeting of The Satellite Division of the Institute of Navigation (ION GNSS 2006)*, Fort Worth, TX, September 2006, pp. 2065–2079.

[21] R. Píriz, D. Calle, A. Mozo, P. Navarro, D. Rodríguez, and G. Tobías, "Orbits and clocks for GLONASS precise-point-positioning," in *Proceedings of the 22nd International Technical Meeting of The Satellite Division of the Institute of Navigation (ION GNSS 2009)*, Savannah, GA, September 2009, pp. 2415–2424.

[22] H. Yamada, T. Takasu, N. Kubo, and A. Yasuda, "Effect of GLONASS orbit error on long baseline GPS/GLONASS RTK," in *Proceedings of the 22nd International Technical Meeting of The Satellite Division of the Institute of Navigation (ION GNSS 2009)*, Savannah, GA, September 2009, pp. 3290–3296.

[23] J. M. Dow, R. E. Neilan, and C. Rizos, "The International GNSS Service in a changing landscape of global navigation satellite systems," *Journal of Geodesy*, vol. 83, pp. 689–689, 2009.

[24] IGS formats, Accessed January 2011. [Online]. Available: http://igscb.jpl.nasa.gov/components/formats.html

[25] Russian Institute of Space Device Engineering, *GLONASS Interface Control Document*, 2008.

[26] CDDIS, Accessed January 2011. [Online]. Available: http://igscb.jpl.nasa.gov/components/dcnav/cddis_data_daily_yyg.html

[27] IGS Products, Accessed January 2011. [Online]. Available: http://igscb.jpl.nasa.gov/components/prods.html

[28] C. Boucher and Z. Altamimi, "ITRS, PZ-90 and WGS 84: current realizations and the related transformation parameters," *Journal of Geodesy*, vol. 75, pp. 613–619, 2001.

[29] *Absolute differences between GLONASS broadcast ephemeris and a posteriori orbits in ITRF system for several orbit slots of the first plane*, Accessed January 2011. [Online]. Available: http://www.glonass-ianc.rsa.ru/docs/PZ-90-2-3-eng.pdf

[30] J. Kouba, *A Guide to Using IGS Products*, IGS, May 2009. [Online]. Available: http://igscb.jpl.nasa.gov/igscb/resource/pubs/UsingIGSProductsVer21.pdf

[31] R. Dach, R. Schmid, M. Schmitz, D. Thaller, S. Schaer, S. Lutz, P. Steigenberger, G. Wbbena, and G. Beutler, "Improved antenna phase center models for GLONASS," *GPS Solutions*, vol. 15, pp. 49–65, 2011.

[32] M. Stewart and M. Tsakiri, "GLONASS broadcast orbit computation," *GPS Solutions*, vol. 2, pp. 16–27, 1998.

[33] A. E. Zinoviev, "Using GLONASS in combined GNSS receivers: Current status," in *Proceedings of the 18th International Technical Meeting of The Satellite Division of the Institute of Navigation (ION GNSS 2005)*, Long Beach, CA, September 2009, pp. 1046–1057.

[34] G. W. Corder and D. I. Foreman, *Nonparametric Statistics for Non-Statisticians: A Step-by-Step Approach*. Wiley, 2009.

[35] H. C. Thode, *Testing for Normality*. New York, NY: Marcel Dekker, 2002.

[36] J. W. Pratt, H. Raiffa, and R. Schlaifer, *Introduction to Statistical Decision Theory*. The MIT Press, 1995.

[37] J. Rife, S. Pullen, B. Pervan, and P. Enge, "Paired overbounding and application to GPS augmentation," in *Proceedings of 2004 IEEE/ION Position Location and Navigation Symposium (PLANS 2004)*, Monterey, CA, April 2004, pp. 439–446.

[38] US DoD, *Global Positioning System Standard Positioning Service Performance Standard*, 4th ed., September 2008.